University of Szeged
Albert Szent-Györgyi Medical School

Doctoral School of Experimental and Preventive Medicine

Cerebral edema evolution and the role of aquaporin-4 in secondary injury after acute ischemic stroke

PhD Thesis

dr. Réka Tóth

Supervisor: Dr. Ákos Menyhárt

Szeged, 2026

Introduction

Stroke affects nearly 94 million people worldwide and remains the second leading cause of death and the third leading cause of death and disability combined. Its global incidence has risen by 70% since 1990, and related mortality and disability have doubled. Beyond the personal and societal burden, annual healthcare spending on stroke approaches 890 billion USD and is expected to double by 2025, underscoring the need for improved therapeutic strategies.

Stroke is defined as an acute focal neurological deficit caused by a disturbance in cerebral circulation. Approximately 87% of cases are ischemic. In acute ischemic stroke (AIS), arterial occlusion abruptly halts blood flow, depriving brain tissue of oxygen and glucose. Loss of Na^+/K^+ ATPase function leads to membrane depolarization and initiates pathological cascades culminating in cell death. The ischemic core, where cerebral blood flow (CBF) falls below 10 ml/100 g/min, undergoes irreversible injury. Surrounding it lies the penumbra, a hypoperfused but potentially salvageable region with CBF between 20–40 ml/100 g/min. Because the penumbra progressively converts into core, rapid reperfusion remains the central goal of AIS therapy in order to salvage the penumbra. However, even successful recanalization does not always prevent delayed infarct progression, and in the last 30 years no new neuroprotective agent has translated from preclinical success to clinical benefit.

Secondary injury mechanisms play a major role in lesion expansion. Among these, spreading depolarizations (SDs)—waves of near-complete neuronal and glial depolarization propagating at 2–6 mm/min—are particularly detrimental. SDs impose extreme metabolic demand and trigger complex vascular responses. In healthy tissue, they evoke transient hyperemia that supports recovery, but in metabolically compromised ischemic cortex, SDs often produce prolonged hypoperfusion called spreading ischemia. This further reduces CBF in already endangered tissue and accelerates penumbra-to-core transformation. SDs also promote cytotoxic edema formation, the first event of cerebral edema concomitant to AIS. In return, cytotoxic cell swelling facilitates further SD generation, creating a self-amplifying cycle of injury.

Cerebral edema (CE) is a major contributor to morbidity and mortality after stroke. Current treatments are largely reactive and target late-stage space-occupying edema, despite cytotoxic edema being the earliest event and a driver of subsequent barrier breakdown. Cytotoxic edema develops within minutes of ischemia, driven by ionic imbalance, Na^+ influx, and water entry into the parenchyma. Vasogenic edema peaks 2–3 days later, following blood–brain barrier (BBB) disruption mediated by inflammatory cascades, allowing protein-rich fluid to accumulate in the extracellular space.

Astrocytes play a central role in edema formation due to their extensive vascular end-feet and expression of aquaporin 4 (AQP4), the

primary water channel in the central nervous system. AQP4 is highly enriched and polarized to perivascular end-feet, providing the base for constant maintenance of cerebral fluid homeostasis. Its importance in cytotoxic edema is demonstrated by AQP4 knockout models, which show ~35% reduction in ischemia-induced swelling. AQP4 expression increases biphasically after stroke, and its membrane localization is regulated by intracellular Ca^{2+} and calmodulin (CaM). Although AQP4 facilitates harmful water influx during edema formation, it also contributes to edema resolution, making direct channel blockade problematic.

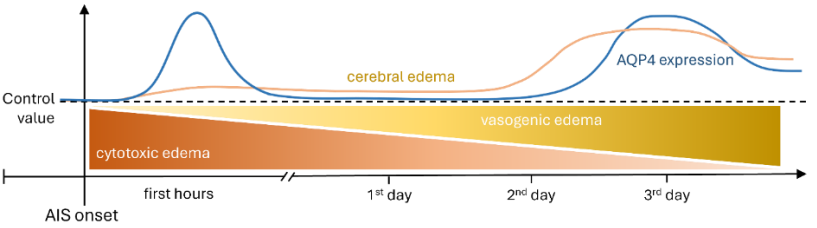

Figure 1. Cerebral edema formation occurs seconds after the onset of ischemia and progresses into vasogenic edema over time, peaking 2-3 days following injury. At the same time, ischemia drives bi-phasic upregulation of the water channel aquaporin-4 (AQP4).

Targeting AQP4 translocation rather than channel function has emerged as a promising strategy. Trifluoperazine (TFP), an FDA approved antipsychotic with CaM inhibitory properties, prevents AQP4 membrane insertion. TFP has been shown to reduce edema and improve outcomes in rodent models of spinal cord injury and photothrombotic stroke, suggesting that modulation of AQP4 trafficking may offer a novel, targeted approach to early edema prevention in AIS.

Hypotheses and aims of the study:

Spreading depolarizations are known to cause cytotoxic astrocytic swelling, which increases tissue susceptibility to subsequent SDs and contributes to astrocyte dysfunction and injury progression. Because AQP4 channels mediate the main route of water entry during early ischemic damage, we aimed to influence AQP4 trafficking by targeting its Ca^{2+}-dependent regulatory pathway through CaM inhibition. The work was structured around the following objectives:

1. Characterization of astrocytic Ca^{2+} dynamics during SDs.
2. Pharmacological suppression of Ca^{2+}-dependent signaling and evaluation of its functional consequences.

Our analyses revealed a paradoxical, non-linear relationship between infarct volume and neurological deficit. This unexpected finding motivated a third, supplementary aim of the thesis.

3. Characterization of the relationship between infarct volume and the corresponding neurological deficit.

Materials and methods

Adult male C57BL/6 mice (2–4.5 months, 26.83 ± 3.91 g) were used. Anesthesia was maintained with isoflurane in O_2:N_2O (1:2; 4% induction, 0.5–1.5% maintenance).

Astrocyte Ca^{2+} Imaging and SD Induction

A 3-mm cranial window was prepared over the right parietal cortex. The brain was loaded with Ca^{2+} indicator dye Fluo-4 AM, followed by sulforhodamine-101 to label astrocytes. A coverslip sealed the craniotomy. A second trepanation allowed SD elicitation via a glass capillary containing 1 M KCl.

Two-photon imaging (FEMTO 3D Dual microscope; 810 nm excitation) was performed at 55–85 µm depth. SDs were triggered every 15–20 min by ejecting 1–3 µL KCl. SD was confirmed by propagating Ca^{2+} waves and characteristic arteriole diameter changes.

SD Susceptibility Testing

In separate mice (n = 18), two craniotomies were made: one for recording and one for SD induction. CBF was monitored with laser Doppler flowmetry, and LFPs were recorded using Ag/AgCl electrodes. After baseline, treated animals (n = 8) received topical 20 µM TFP; controls (n = 10) received solvent. SDs were elicited with 1 M KCl every 15 min for 120 min.

Transient middle cerebral artery occlusion (MCAO)

Ischemic stroke was induced by 60-min intraluminal filament occlusion of the left MCA (n = 69). CBF reduction to <20% confirmed occlusion. Reperfusion was achieved by filament withdrawal and sealing the carotid puncture. The operation was followed by 72 hour survival period,

Postoperative Care and Treatment

Animals received carprofen (5 mg/kg, every 12 h), glucose-saline and Duphalyte-saline supplements, and soft food. Two TFP regimens were tested: 1 mg/kg at reperfusion and every 24 h (n = 14), or a single 5 mg/kg dose at reperfusion (n = 13). Controls received saline (n = 14). Fourteen mice were excluded due to early death.

Functional Testing and Imaging

Neurological deficits were assessed using the Garcia Neuroscore from 24–72 h. Neurovascular coupling (n = 19) was evaluated by whisker stimulation and CBF recording. MRI and SPECT (n = 21) were performed at 72 h; [^{99m}Tc]DTPA (76.03 ± 34.23 MBq) was injected 2 h before SPECT. T2-weighted, diffusion-weighted MRI and ADC maps were used to calculate lesion and hemispheric volumes.

Results

Astrocyte Ca^{2+} oscillations follow the Ca^{2+} wave of SD

Topical application of 1 M KCl reliably triggered spreading depolarization (SD), confirmed by the characteristic propagation velocity of the astrocytic Ca^{2+} wave (77.5 ± 25.2 µm/s). After the synchronized Ca^{2+} wave, the same astrocyte network exhibited delayed, non synchronized Ca^{2+} oscillations with an average onset delay of 183.64 ± 89.21 s. These oscillations occurred at a frequency of 0.66 ± 0.32 events/min/cell, approximately three times higher than spontaneous baseline activity (0.19 ± 0.032 events/min/cell). The oscillations were random, repetitive, and showed no temporal coincidence between cells. Their peak fluorescence amplitude was significantly smaller than that of the preceding Ca^{2+} wave (54.02 ± 22.65 vs. 98.06 ± 24.35 ΔF/F).

TFP enhances the CBF response to SD in the non-ischemic cortex

We next examined the effect of the CaM inhibitor TFP on SD characteristics and associated vascular responses. TFP tended to reduce both the frequency and amplitude of KCl-induced SDs (12.96 ± 7.05 vs. 18.88 ± 2.64 mV, TFP vs. control), although not significantly. TFP did not alter the CBF response to the first SD (118.9 ± 22.7 vs. 112.7 ± 23.5 %, TFP vs. control). However, during recurrent SDs, CBF responses exceeded baseline in the TFP group (122.6 ± 23.5 %), but remained below it in controls (93.6 ± 26.7 %). This difference was most pronounced in the hyperemic AUC (9419.4 ± 2173.6 vs. 5444.7 ± 1828.2 %×s; TFP vs. control).

Verification of ischemic lesion formation after transient MCAO

Successful MCAO was confirmed by laser Doppler flowmetry, showing a drop in perfusion to 13.11 ± 6.00 % of baseline, consistent with ischemic core levels. MRI performed 72 h after MCAO verified lesion formation, with lesion volumes (LVs) ranging from 17–130 mm^3, corresponding to 7.31–54.17 % of the hemisphere (HLV%: 35.71 ± 12.06 %). T2 hyperintense regions consistently overlapped with areas of restricted diffusion on ADC maps ($5.01 \pm 0.32 \times 10^{-4}$ vs. $7.89 \pm 0.60 \times 10^{-4}$ mm^2/s; lesion vs. intact hemisphere).

Progression of cerebral edema compromises LV estimation

Cerebral edema significantly distorted LV estimation. Hemispheric swelling correlated with apparent LV enlargement ($R = 0.724$,

$p = 0.0023$). The affected hemisphere expanded by 17.32 ± 12.39 % (%HSE), and swelling correlated with LV increase ($R = 0.705$, $p = 0.003$). Edema corrected lesion volumes (LVc) were therefore calculated, reducing LV estimates from 87.13 ± 30.64 mm³ to 44.36 ± 23.56 mm³.

Lesion volumes display no relationship with GNS

Sensorimotor function was assessed using the GNS score. Neither raw nor corrected lesion volumes correlated with GNS at the time of MRI ($R = 0.0581$, $p = 0.837$; $R = 0.167$, $p = 0.552$). LVc also showed no correlation with GNS at 24 h ($R = 0.170$, $p = 0.545$), 48 h ($R = 0.0808$, $p = 0.775$), or 72 h ($R = 0.058$, $p = 0.837$). In contrast, GNS at 24 h strongly predicted GNS at 72 h ($R = 0.748$, $p = 0.0013$).

Paradoxical association LVs with neurological impairment

Three of the 15 mice displayed a paradoxical pattern: markedly smaller LVc (14.64 ± 6.25 mm³ vs. 51.79 ± 19.96 mm³) despite severe neurological deficits (GNS 72 h: 9 ± 2 vs. 11 ± 2). Although 12/15 mice showed LV–GNS compatibility, the LVc–GNS relationship weakened by day 3 ($R = 0.146$, $p = 0.61$ vs. $R = 0.485$, $p = 0.110$ at 24 h). Excluding atypical cases did not improve correlations ($R = 0.298$, $p = 0.92$). Brain swelling also showed no association with GNS ($R = 0.235$, $p = 0.398$), indicating that neither lesion size nor edema alone explains functional deficits.

TFP treatment decreases lesion size

MRI at 72 h revealed cortical and striatal infarcts in all groups. Only the higher single TFP dose administered at recanalization significantly reduced lesion size (52.51 ± 15.56 vs. 31.98 ± 14.46 vs. 20.51 ± 15.61 mm³; control vs. TFP1 vs. TFP5). Despite smaller lesions, hemispheric swelling remained comparable across groups (20.91 ± 14.91 % vs. 25.35 ± 5.74 % vs. 21.07 ± 6.33 %).

SPECT imaging showed increased DTPA uptake in all stroke-affected regions, with no significant differences between groups in SUV (558.00 ± 185.78 % vs. 820.86 ± 285.66 % vs. 632.33 ± 247.14 %; $p = 0.126$) or lesion area (75.74 ± 25.16 vs. 82.14 ± 17.95 vs. 78.59 ± 18.81 mm³; $p = 0.846$).

TFP improves neurovascular coupling and functional outcome

Functional hyperemia was markedly reduced in the MCA territory after stroke (4.01 ± 3.77% vs. 22.39 ± 9.48%). TFP significantly improved hyperemia (20.65 ± 8.80% and 19.49 ± 11.93% for TFP1 and TFP5), restoring responses to near-intact levels. Treated animals also performed better in functional tests on postoperative days 2&3.

Discussion

The aim of our work was to determine whether limiting early edema formation after ischemic stroke can reduce infarct size and improve sensorimotor outcomes. To address this, we targeted a Ca^{2+} dependent

signaling pathway in astrocytes that regulates the intracellular trafficking of AQP4, the main water channel in the brain.

In the first phase of the study, we studied astrocytic Ca^{2+} dynamics associated with spreading depolarization (SD) in the anesthetized mouse somatosensory cortex. Beyond confirming the transient Ca^{2+} elevations that accompany SD, we represent the first in vivo demonstration of delayed astrocytic Ca^{2+} oscillations following SD. These oscillations appeared 2–4 minutes after the SD related Ca^{2+} wave and occurred at a frequency of 0.66 ± 0.32 events/min/cell, approximately three times higher than spontaneous baseline fluctuations and appeared as unsynchronized oscillatory activity across cells. The oscillations also showed smaller amplitude than the preceding Ca^{2+} wave, suggesting distinct underlying mechanisms. While SD related Ca^{2+} waves likely rely on multiple pathways involving extracellular Ca^{2+} entry, the delayed oscillations may primarily reflect Ca^{2+} release from intracellular stores such as the endoplasmic reticulum or mitochondria.

Among the channels contributing to Ca^{2+} influx during SD, TRPV4 plays a central role. TRPV4 is a non selective cation channel with high Ca^{2+} conductance, enriched in astrocytic endfeet where it forms a functional complex with AQP4. Importantly, TRPV4 and AQP4 exhibit strong functional interdependence: deletion of either disrupts the function of the other. Ca^{2+} influx through TRPV4 stabilizes the interaction between AQP4 and calmodulin (CaM), promoting CaM

dependent AQP4 translocation to the plasma membrane. Because our experiments confirmed dynamic Ca^{2+} changes capable of triggering this pathway, we next examined whether pharmacological interference could mitigate early edema.

In the second phase, we tested trifluoperazine (TFP), a CaM inhibitor previously shown to block AQP4 translocation. We hypothesized that TFP would reduce cytotoxic edema during the acute phase of ischemia, limit infarct maturation, and improve neurological and cerebrovascular outcomes. AQP4 is known to play a dual, phase dependent role in stroke: it contributes to early cytotoxic edema but later facilitates vasogenic edema clearance and glymphatic drainage. While AQP4 knockout studies show reduced early edema, they also report increased hemispheric swelling several days after MCAO. Thus, therapeutic targeting of AQP4 requires precise timing. TFP is an attractive candidate, because it alters AQP4 localization without permanently inhibiting its function.

Contrary to expectations, neither bolus nor repeated TFP administration reduced edema volume. However, infarct size was significantly reduced, and neurological outcomes improved, particularly when TFP was delivered as a single dose immediately after recanalization. We propose that TFP effectively mitigates early cytotoxic edema and neuronal injury, but MRI performed three days after MCAO primarily reflects delayed vasogenic edema, which TFP does not influence. This interpretation is supported by our SPECT

findings showing no effect of TFP on BBB leakage. Despite this, TFP clearly exerted neuroprotective effects, reducing infarct volume and improving functional recovery.

TFP also markedly improved neurovascular coupling in ischemic tissue and enhanced the CBF response to SD in normally perfused cortex. Astrocytes are central regulators of SD related vascular responses, and SD itself induces astrocytic swelling. Swollen astrocytic endfeet compress microvessels, impairing perfusion. By preventing AQP4 translocation and reducing astrocytic swelling, TFP may relieve this mechanical compression and restore cerebrovascular function. Alternatively, ischemia induced edema may disrupt astrocytic vasoactive signaling, and TFP may shift the balance toward vasodilation by suppressing vasoconstrictor pathways or rescuing vasodilator mechanisms.

During MRI analysis, we frequently observed pronounced hemispheric swelling three days after MCAO. This phenomenon is well documented in both animal models and stroke patients, particularly after successful recanalization, when restored blood flow drives water influx through damaged capillaries. Because edema expands lesion volume, we applied edema correction to more accurately assess infarct size. Although large swelling volumes predict poor outcome clinically, edema alone did not explain the neurological deficits in our study.

We also identified a discrepancy between infarct size and neurological impairment in the MCAO model. Our findings show that infarct volume alone is not a reliable predictor of sensorimotor deficits. Similar inconsistencies have been reported clinically and may contribute to the translational gap in stroke research. Rodent MCAO models exhibit substantial variability in infarct size, and early imaging based predictions depend heavily on timing and occlusion duration. Additional explanations include infarct localization effects and the clinical DWI mismatch phenomenon, where severe symptoms accompany minimal early imaging abnormalities, possibly indicating evolving secondary injury processes. Overall, the paradoxical relationship between lesion volume and functional deficit underscores the need for more nuanced outcome measures in both experimental and clinical stroke research.

Acknowledgements

I consider myself a lucky person indeed, as I've always had the chance to work in fields that genuinely interest me and have always been fond of my job. As a result - as the saying goes - I feel as though I haven't really had to work a single day in my life so far. This would not have been possible without some truly exceptional people. I am sincerely grateful to Prof. Dr. Eszter Farkas for believing in me from the very beginning and supporting all my ideas, and to my supervisor, Dr. Ákos Menyhárt, whose enthusiasm and guidance created a motivating, cheerful environment filled with both science and humour. I also thank Prof. Dr. Ferenc Bari for supporting our group and our work. I am deeply grateful to my lab members, especially Dr. Anna Törteli for sharing this PhD journey and becoming a true friend, and to Dr. Rita Frank for always being a kind, protective presence. I thank my family

for their unwavering love and support, and my friends - those from the beginning and those met along the way - who are pure joy and who always patiently listened to my endless gushing about astrocytes.

Articles to serve as the basis of the thesis

1. **Tóth R**, Farkas AE, Krizbai IA, Makra P, Bari F, Farkas E, Menyhárt Á. *Astrocyte Ca^{2+} Waves and Subsequent Non-Synchronized Ca^{2+} Oscillations Coincide with Arteriole Diameter Changes in Response to Spreading Depolarization.* **International Journal of Molecular Sciences** 2021 Mar 26;22(7):3442. doi: 10.3390/ijms22073442. PMID: 33810538; PMCID: PMC8037646. **IF: 6.2**

2. **Tóth R**, Szabó N, Törteli A, Kovács N, Horváth I, Szigeti K, Máthé D, Kincses TZ, Menyhárt Á, Farkas E. *The paradoxical relationship of sensorimotor deficit and lesion volume in acute ischemic stroke*. **Journal of Neuropathology & Experimental Neurology** 2025 Sep 1;84(9):771-779. doi: 10.1093/jnen/nlaf046. PMID: 40272944; PMCID: PMC12365491. **IF: 2.9**

3. **Tóth R**, Törteli A, Szabó M, Kovács N, Horváth I, Farkas A, Frank R, Szigeti K,
   Bari F, Krizbai IA, Máthé D, Menyhárt Á, Farkas E.
   Trifluoperazine reduces infarct size, restores neurovascular coupling and improves early outcomes in experimental acute ischemic stroke
   Currently under review at Journal of Cerebral Blood Flow and Metabolism, 2026